JACEK KŁOSIŃSKI[*)]

SLEWING MOTION CONTROL IN MOBILE CRANE ENSURING STABLE POSITIONING OF CARRIED LOAD

The author presents an algorithm of slewing motion control in telescopic crane mounted on a chassis of a truck (mobile crane). The control algorithm allows the crane to carry load to a selected point, and it also ensures suppression of swing at the endpoint of the motion. The attention was focussed mainly on the control of slewing motion of the crane body in the case of non-planar distribution of forces acting on the load during its motion.

1. Introduction

In general, the aim of working motion control in mobile cranes is to carry a load (payload) from one point to another while preventing the load from excessive swinging at the endpoint. The swing-free termination of the load motion (with assumed precision of position co-ordinates and their derivatives) is called load positioning. In order to ensure proper load positioning, the strategy applied to control the motion of load suspension point must meet specific requirements. These involve proper composition of working motions, and must take into account the time-function of trajectory of the load suspension point. Both conditions influence the magnitude of swing appearing during working motion. However, the trajectory function is the most important factor to be considered in designing the control strategy.

In this paper, the author presents an algorithm of slewing motion control in telescopic crane mounted on a chassis of a truck. The control algorithm allows the crane to carry load to a selected point, and at the same time ensures suppression of swing at the end of the motion. Attention was focussed mainly on the control of slewing motion of the crane body. The reason was non-planar distribution of forces acting on the load during its motion. To deal with this

[*)]   *Technical University of Łódź, Branch in Bielsko-Biała; ul. Willowa 2, 43-309 Bielsko-Biała Poland; E-mail: jklosinski@pb.bielsko.pl*

problem, one developed simplified models of the crane and the hydraulic drive system. Then, analytical identification of both models was performed. Treating the two models as controlled objects, one proposed the structure of the system aimed at controlling the component of load oscillation tangential to the circular trajectory drawn by the load suspension point (head of the jib) in its working motion. As the slewing motion of the body is considered, the system concerned controls the component of swing tangential to the circle drawn by the suspension point in its motion around the vertical axis. In the schematic diagram of the model (Fig. 1) this component is denoted by symbol v.

Once an appropriate control unit was accepted, and the input signal function in the control system was calculated (or assumed), one performed numerical simulation of the whole control system. In the case when the input signal is a decaying function, the system will tend to liquidate the tangential component of load swing. Proper choice of the input signal function can also ensure reduction of the second, radial component of the swing – that perpendicular to the tangential one. The numerical simulations, performed by the author, made it possible to evaluate the model's sensitivity to disturbances, find the values of control unit settings and determine the form of the input signal. The undertaking was complemented by an experiment on a physical model of the crane. The purpose of the experiment was to verify the control strategy in the aspect of its technical usability.

2. Mathematical model of control system of slewing motion of crane body

2.1. Identification of controlled object

2.1.1. Mathematical model of slewing motion of crane body

After reviewing and analysing crane models known from literature [2], [3], [11], the author proposed a three-dimensional, discrete model of slewing motion of crane body based on the following assumptions:

- The solids of chassis and body, of known masses and moments of inertia, are rigid and have six degrees of freedom;
- One neglects vertical dislocations of elements; the only possible motion of the body is its rotation about the axis attached to immobile chassis;
- The system of outriggers is replaced by a system of springs; mass of outriggers is neglected;
- The crane body is rotated by means of a hydrostatic drive system through a mechanical gear of known rigidity; the centre of body's mass lies on the axis of rotation of the body;
- The jib is treated as a rigid rod of constant length, of known mass and moment of inertia; it is connected with the body by means of a cylindrical joint allowing only for the change of jib's inclination angle;

- The load hangs on an inextensible, weightless, whippy cable of constant length; the hanging load can be treated as a spherical pendulum;
- One assumes that movements of masses, described by generalised co-ordinates, are small, except of those resulting from slewing motion of the body;
- Friction and shake is neglected in all elements of the support system, jib, and mechanical gear;
- Damping in the system is neglected;
- One assumes linearity of characteristics of elastic constraints.

Schematic diagram of slewing motion of crane body is presented in Fig. 1 [5].
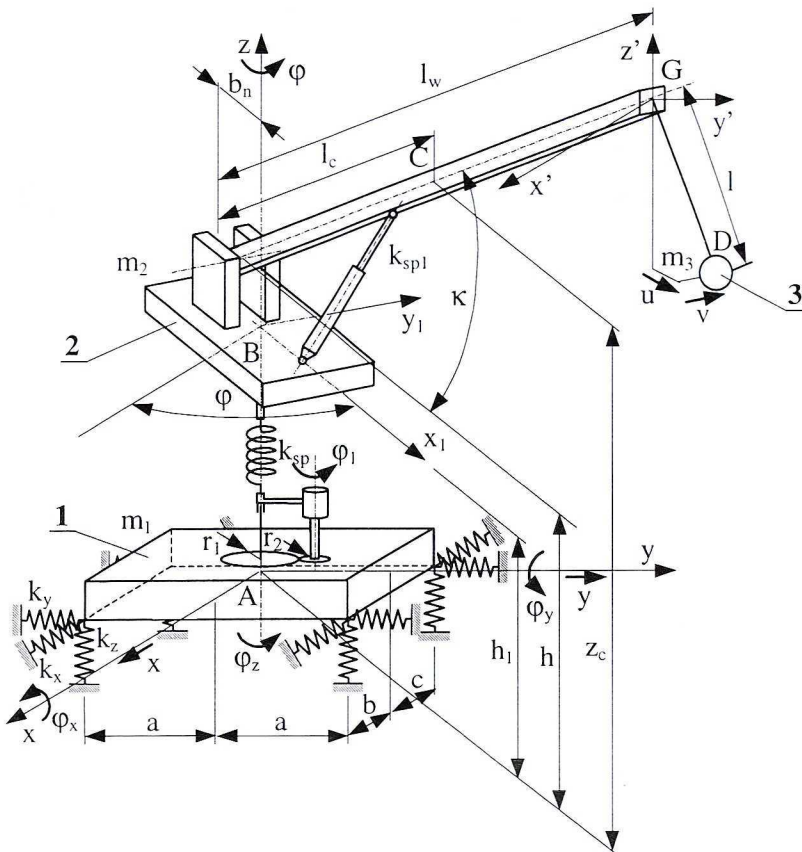
Fig. 1 Schematic diagram of mobile crane. 1– chassis, 2 - body with jib, 3 – load, k_{sp}, k_{sp1}, k_x, k_y, k_z – rigidity coefficients of elastic elements assumed in the model, h_1, z_c - height of the position of centre of mass of body and jib, respectively, in reference to chassis centre of mass, h - height of the position of jib axis of rotation, κ - inclination angle of jib axis in reference to horizontal plane.

Generalised co-ordinates of the model are denoted by vector $\mathbf{q_1}$ consisting of the following n components (n=8)

$$\mathbf{q_1} = \begin{bmatrix} x & y & u & v & j & j_x & j_y & j_z \end{bmatrix}^T,$$
(1)

where

x, y — linear dislocations of the body centre of mass referred to a fixed reference system;

u, v — projections of load dislocations onto horizontal plane in the radial direction, and tangential direction, respectively, in the circle described by jib's head; these components are determined in a movable system, rotating with the jib;

φ — angle of rotation of the body and the jib about vertical axis;

$\varphi_x, \varphi_y, \varphi_z$ — angles of rotation (oscillation) of the crane in reference to axes connected with the centre of mass of the body;

The total kinetic energy of the system was calculated as the sum of kinetic energies of chassis, body with jib and load, according to the formula:

$$E_k = \sum_i E_{ki} = \frac{1}{2} \sum_{i=1}^{n_1} \left[\mathbf{v}_{si}^T m_i \mathbf{v}_{si} + \boldsymbol{\omega}_i^T \mathbf{J}_i \boldsymbol{\omega}_i \right] = \frac{1}{2} \dot{\mathbf{q}}_1^T \mathbf{M}_1 \dot{\mathbf{q}}_1,$$
(2)

where

$\mathbf{v}_{si}$ — velocity vector of centre of mass of ith element, related to a stationary system of co-ordinates,

$\boldsymbol{\omega}_i$ — angular velocity vector of ith element defined in reference to element's centre of mass,

m_i — mass of ith element,

$\mathbf{J}_i$ — diagonal matrix of moments of inertia of ith element in the system of co-ordinates connected with element's centre of mass,

n_1 — number of individual elements ($n_1 = 3$),

$\mathbf{M}_i$ — symmetrical square matrix (n×n) whose elements are functions of masses and moments of inertia of model elements, and depend on generalised co-ordinates; the matrix is presented in detail in the Appendix.

Potential energy of the system is the sum of potential energies of masses in the gravitational field, and potential energy of deformed elastic constraints. It can be expressed by the formula:

$$E_p = \mathbf{G}^T \mathbf{z}_s + \frac{1}{2} \mathbf{w}^T \mathbf{C} \mathbf{w} = \frac{1}{2} \mathbf{q}_1^T \mathbf{C}_{p1} \mathbf{q}_1 + \mathbf{c}_{r1}^T \mathbf{q}_1 + c_{s1}$$
(3)

where

$\mathbf{G}$ — vector of gravity forces;

$\mathbf{z}_s$ — vector of co-ordinates of element centres of masses related to a selected reference point (centre of chassis mass, for instance);

$\mathbf{w}$ – deflection vector of deformable elastic constraints;

$\mathbf{C}$ – matrix of rigidity of linear elastic constraints (in the model, this matrix contains rigidity of springs modelling flexibility of support system, jib and driving gear)

$\mathbf{C_{p1}}$ – symmetrical square matrix (n×n) whose elements are functions of rigidity coefficients of selected elastic elements in the model, and depend on masses and generalised co-ordinates;

$\mathbf{c_{r1}}$ – n-dimensional vector whose components are functions of masses, rigidity coefficients and generalised co-ordinates;

c_{s1} – scalar quantity that is also a function of the above mentioned variables; full expressions of $\mathbf{C_{p1}}$, $\mathbf{c_{r1}}$ and c_{s1} are included in the Appendix.

Next, one calculates derivatives of kinetic energy (2) with respect to generalised velocities and time,

$$\frac{d}{dt}\left(\frac{\partial E_k}{\partial \dot{\mathbf{q}}_1}\right) = \frac{d}{dt}(\mathbf{M}_1\dot{\mathbf{q}}_1) = \frac{d\mathbf{M}_1}{dt}\dot{\mathbf{q}}_1 + \mathbf{M}_1\ddot{\mathbf{q}}_1 \qquad (4)$$

as well as derivative with respect to generalised co-ordinates:

$$\frac{\partial E_k}{\partial \mathbf{q}_1} = \frac{1}{2}\left(\dot{\mathbf{q}}_1^{\mathrm{T}}\frac{d\mathbf{M}_1}{d\mathbf{q}_1}\right)\dot{\mathbf{q}}_1 = \frac{1}{2}\mathbf{L}_1\dot{\mathbf{q}}_1 \ , \qquad (5)$$

and finally derivative of potential energy (3) with respect to generalised coordinates:

$$\frac{\partial E_p}{\partial \mathbf{q}_1} = \mathbf{C}_{p1}\mathbf{q}_1 + \frac{1}{2}\left(\mathbf{q}_1^{\mathrm{T}}\frac{d\mathbf{C}_{p1}}{d\mathbf{q}_1}\right)\mathbf{q}_1 + \mathbf{c}_{r1} + \frac{d\mathbf{c}_{r1}}{d\mathbf{q}_1}\mathbf{q}_1 + \frac{dc_{s1}}{d\mathbf{q}_1} =$$
$$= \left(\mathbf{C}_{p1} + \frac{1}{2}\mathbf{L}_2 + \mathbf{L}_3\right)\mathbf{q}_1 + \mathbf{c}_{r1} + \frac{dc_{s1}}{d\mathbf{q}_1} \ , \qquad (6)$$

where

$\mathbf{L}_i$ – square matrices of dimensions n×n (for i=1, 2, 3), whose form results from formulas (5) and (6).

Substituting expressions (4), (5) and (6) into Lagrange's equation of type II, one obtains, on the assumption of negligible damping in the system, the following nonlinear matrix differential equation:

$$\mathbf{M}_1\ddot{\mathbf{q}}_1 = \mathbf{P}_1 \ , \qquad (7)$$

where

$$\mathbf{P}_1 = -\frac{d\mathbf{M}_1}{dt}\dot{\mathbf{q}}_1 + \frac{1}{2}\mathbf{L}_1\dot{\mathbf{q}}_1 - \left(\mathbf{C}_{p1} + \frac{1}{2}\mathbf{L}_2 + \mathbf{L}_3\right)\mathbf{q}_1 - \mathbf{c}_{r1} - \frac{dc_{s1}}{d\mathbf{q}_1} + \mathbf{F}_1 = \mathbf{f}_1(\mathbf{q}_1, \varphi_1, t)$$

$\mathbf{P_1}$ – n-dimensional vector whose components are functions of generalised co-ordinates and their derivatives,

$\mathbf{F_1}$ – vector of generalised forces pertaining to generalised co-ordinates,

φ_1 – shaft rotation angle in hydraulic drive engine.

Equation (7) is the matrix equation of motion of crane model describing the rotation movement of crane's body, in which the shaft rotation angle of hydraulic drive engine $\varphi_1(t)$ is the input control signal, and the component tangential to load swing $v(t)$ is the output of control system. There is

$$v = \mathbf{c_1^T q_1},\tag{8}$$

where

$$\mathbf{c_1} = [0\ 0\ 0\ 1\ 0\ 0\ 0\ 0]^T.$$

In the block diagram (Fig. 3) this equation describes the block named "Crane Model".

2.1.2. Mathematical model of hydraulic drive system

A hydrostatic drive system, applied in the crane, allows the crane body to perform the slewing motion. The system comprises hydraulic engine of constant absorbing capacity with a proportional valve used as the element that throttles the flow of oil. Fig. 2 presents schematic diagram of the system model on which dynamical analysis was performed.
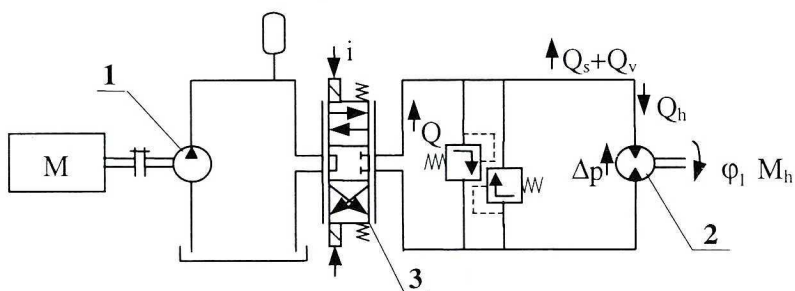
Fig. 2 Schematic diagram of hydraulic drive system of mobile crane. 1 – pump, 2– hydraulic engine, 3 –electro-hydraulic proportional valve

In the development of the hydraulic system model of crane body rotational mechanism, one takes the following assumptions:

• pump delivery is constant, and so is the engine absorbing capacity,

• the pressure in pump pressure conduit is constant,

• the valve has zero overlap,

- there exist volumetric losses in the system,
- oil compressibility and flexibility of oil conduits are taken into account,
- one takes into account the throttling effect in the control valve (the effect consists in decreasing flow intensity with the increase of pressure drop on the engine [10]),
- moments of inertia of moving parts of the engine are neglected,
- both the engine and the valve are linear elements,
- oil temperature in the hydraulic system is constant,
- the safety-valve and the overflow valve are in the state of closure.

The mathematical model of the system shown in Fig. 2 is obtained on the basis of the equation of balance of flow intensity in hydrostatic system elements [4], [10].

$$Q = Q_h + Q_s + Q_v , \qquad (9)$$

where

Q – intensity of fluid flow through hydro-electric valve,

$Q = k_s i - k_t \Delta p$,

i – control current in solenoid valve,

Q_h – absorbing capacity of hydraulic engine,

$Q_h = k_h \dfrac{d\varphi_1}{dt}$,

Q_v – volumetric losses in the system,

$Q_v = k_v \Delta p$,

Q_s – losses of fluid resulting from its compressibility and flexibility of the system,

$Q_s = k_c \dfrac{d\Delta p}{dt}$,

Δp – pressure drop on engine,

$\Delta p = \dfrac{M_h}{k_M}$,

M_s – moment produced by hydraulic engine,

$M_h = k_{sp} \left(\varphi_1 - \dfrac{\varphi}{i_p} \right)$,

k_s, k_t, k_M, k_h, k_t, k_v, k_{sp} – coefficients denoting: amplification of intensity of fluid flow through valve at zero pressure drop on engine, valve throttling effect, moment produced by hydraulic engine, absorbing capacity of engine, fluid compressibility, volumetric losses and equivalent rigidity of jib and mechanical gear in rotational drive transmission of the system, respectively,

i_p – kinematic position of drive gear.

After substituting all the formulae into equation (9) and applying some transformations one obtains:

$$\dot{\varphi}_1 = \frac{1}{k_1}\left[k_s i + \frac{k_c k_{sp}}{k_M i_p} \dot{\varphi} - \frac{k_t + k_v}{k_M} k_{sp}\left(\varphi_1 - \frac{\varphi}{i_p} \right) \right] = f_2(\mathbf{q}_1, \varphi_1, i, t), \qquad (10)$$

where

$$k_1 = \frac{k_h k_M + k_c k_{sp}}{k_M}.$$

Equation (10) represents the model of drive system, in which the control current i(t) of the solenoid valve is the input signal, and the angle of rotation of hydraulic engine shaft $\varphi_1 = (t)$ is the output signal. In the block diagram (Fig. 3) this equation describes the block named "Hydrostatic Drive System".

2.2 Synthesis of control system

The system of control of crane's body slewing motion is designed as a system with an auxiliary controlled quantity (UPWR). The structural block diagram of the system is presented in Fig. 3.
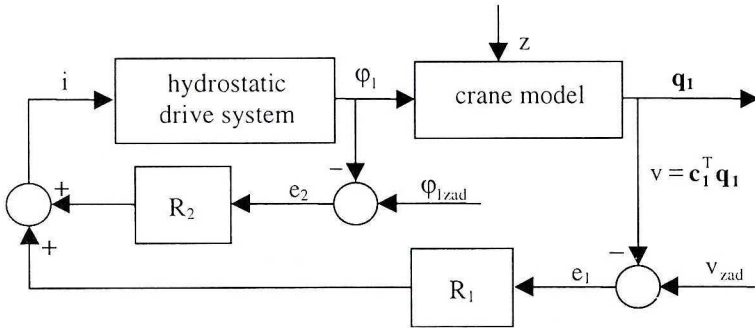
Fig. 3 Block diagram of crane control system

It includes two control loops: the fast one, with control unit R_2, used to control angular position of the hydraulic engine, and the loop with control unit R_1 appropriated to controlling a selected generalised co-ordinate in the crane model. In most cases, this co-ordinate is the tangential component of load swing, v. In the case when one of the control units is switched off, the structure of the system simplifies, and one obtains:

− For $R_2 = 0$ − closed-loop system of control of swing component v; when one applies the control strategy aimed at minimising load swing at the end of working motion, this one can be called the system for suppressing (minimising) tangential component of the swing (ULW).

- For $R_1 = 0$ – closed-loop system of control of angular position of hydraulic engine shaft (URP), whose output signal $\varphi_1(t)$ controls, in an open loop, the element representing crane model.

According to block diagram of Fig 3, the equations of summation nodes can be written as:

$$e_1 = v_{zad} - v = v_{zad} - \mathbf{c}_{e1}^T \mathbf{q}_1 \ ,$$
$$e_2 = \varphi_{1zad} - \varphi_1 \ , \tag{11}$$

where

  $v_{zad}, \varphi_{1\,zad}$ – input signals in control system,
  $\mathbf{c}_{e1}$ – vector of coefficients; for the vector $\mathbf{q}_1(1)$ there is $\mathbf{c}_{e1} = \mathbf{c}_1$, according to (8).

Assuming specific type of control units in the system (PID, for instance) one can, on the basis of the model of crane body slewing motion (7), (8) and the driving system model (10), create a model of the closed-loop control system UPWR in the form of second-order nonlinear matrix equation

$$\mathbf{M}_{r1}\ddot{\mathbf{q}}_{r1} = \mathbf{P}_{r1} \tag{12}$$

where

  $\mathbf{M}_{r1}$ – matrix consisting of elements of matrix $\mathbf{M}_1$ (2), and some of the coefficients of equation (1) and equations describing control unit characteristics,

  $\mathbf{q}_{r1} = \begin{bmatrix} \mathbf{q}_1 \\ \varphi_1 \end{bmatrix}$ – vector of generalised co-ordinates of slewing motion of

  crane body, complemented with the co-ordinate φ_1 describing angle of rotation of the shaft in drive system,

  $\mathbf{P}_{r1}$ – vector of forces and mutual couplings consisting of elements of vector $\mathbf{P}_1$ (7) and parameters of input signals v_{zad} and $\varphi_{1\,zad}$.

After some transformations, equation (12) takes the form

$$\ddot{\mathbf{q}}_{r1} = \mathbf{f}(\mathbf{q}_{r1}, \dot{\mathbf{q}}_{r1}, t) + \mathbf{B}\mathbf{r}_1 \tag{13}$$

where:

  $\mathbf{B} = [\mathbf{b}_1\ \mathbf{b}_2]$ – two-column matrix of coefficients ($\mathbf{b}_2 = \mathbf{0}$ for ULW, and $\mathbf{b}_1 = \mathbf{0}$ for URP),
  $\mathbf{r}_1 = [v_{zad}(t),\ \varphi_{1\,zad}(t)]^T$ – vector of input control signals in the system.

Therefore, equation (13) makes up the mathematical model of the whole control system UPWR.

2.3. Selection of input signal function in control system

The choice of proper signal function in the control system designed to suppress load swing at the end of crane working motion can be based on the analysis of similar signals in control systems used in the cranes where load

moves in a planar motion, like in overhead or gantry cranes. In the case of zero initial conditions, the waveform of control signal can be divided into three phases. In the first one, the load suspension point (the point at which the hoisting rope is attached to the jib) is accelerated to a certain speed. In the second phase, this point travels with approximately constant velocity, and in the third one the point decelerates until its velocity drops to zero.
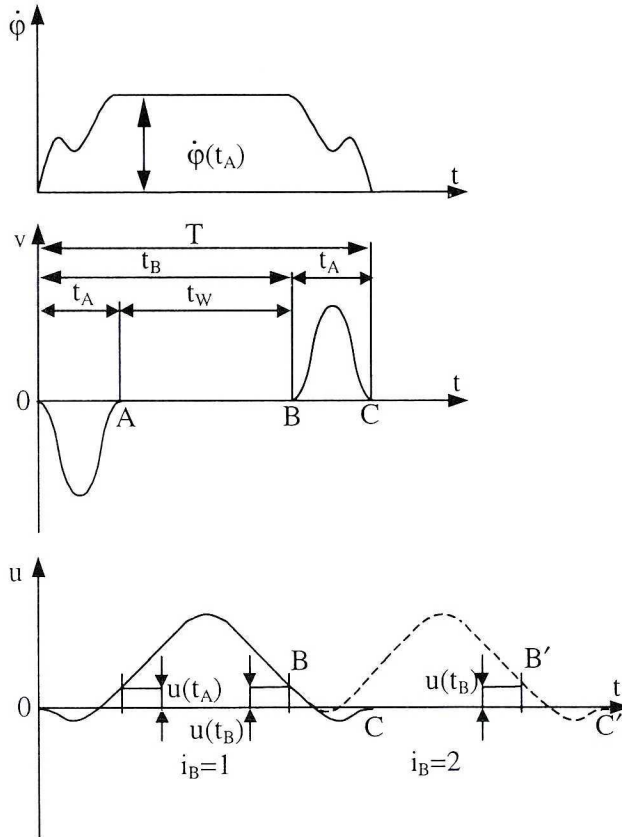
Fig. 4 Waveforms of rotational speed of the jib and of load swing components

During the first phase of the motion, the expected function of tangential component of load swing should take the form (Fig. 4) that obeys the following conditions:

$$v(0) = 0 \, ,$$
$$v(t_A) = v_A \, , \tag{14}$$
$$v \leq 0 \ \text{for} \ t \in [0, t_A] \, ,$$

where:

t_A – time of duration of the first phase of movement; usually t_A depends on rope length, l (Fig. 1),

v_A – the value of tangential component at $t=t_A$; in the case of global balancing of swing [1], and in working motions that does not ensure planar motion of the load, $v_A=0$.

The presence of the second phase of the motion is demanded mainly for safety reasons, and for the purpose of limiting excessive speed of load transport. It should be characterised by the following requirements concerning the functions of load swing components (Fig. 4):

$$v(t_B) = -v(t_A) \ ,$$
$$u(t_B) = u(t_A) \ , \qquad\qquad (15)$$
$$\mathrm{sgn}\left(\left.\frac{du}{dt}\right|_{t=t_B} \right) = - \ \mathrm{sgn}\left(\left.\frac{du}{dt}\right|_{t=t_A} \right),$$

where:

$t_B = t_A + t_W$,

t_W – duration time of the second phase; in the case of local balancing of swing [1], and in working motions that does not ensure planar motion of the load, t_W is a function of rope length l (one can also accept the possibility of $t_W=0$).

The third phase of the motion is, in most cases, reciprocal to the first one. It should then be characterised by the following requirements:

$$v(t_B) = -v_A \ ,$$
$$v(T) = 0 \ , \qquad\qquad (16)$$
$$v \geq 0 \ \text{for} \ t \in [t_B, T] \ ,$$

where:

$T = t_A + t_B = 2t_A + t_W$ – duration time of working cycle.

Application of the conditions (14), (15), (16) to the function of input signal $v_{zad}(t)$ in the control system ULW (Fig. 3; $R_2 = 0$) makes it possible to perform the working motion and, at the same time, suppress load swing. The presence of various disturbances in the crane model can make suppression of the radial (perpendicular to v) component of load swing imperfect. The form of function v_{zad}, in consecutive phases of the motion, can be calculated by solving appropriately formulated boundary conditions [6], [7], [16], or it can be assumed [3], [15]. Simulation tests, done by numerical methods, have shown that sensitivity of the system ULW to the form of input control function v_{zad} is relatively low, provided settings of control unit R_1 are correct.

By numerical simulation of performance of the control system ULW, one obtains time functions of all the co-ordinates that appear in the models of crane and drive system, in particular, the function of rotation angle of engine shaft $\varphi_1(t)$. The time function, calculated in such a way, can be used as the input

signal $\varphi_{1\ zad}(t)$ in the system URP that controls angular position of the engine shaft. The system URP with such an input signal, connected in series with the crane model (Fig. 3; $R_1=0$), guarantees suppression (minimisation) of tangential component of load swing at the end of working motion (if no disturbances are present there).

3. Numerical and experimental examination of control system of crane body slewing motion

A number of numerical simulations of models of control systems of crane body slewing motion were carried out to examine model's sensitivity to the form of input signal function $v_{zad}(t)$, disturbances in the system appearing in the form of random forces acting on the load during its motion, the values of kinematic-geometric parameters characterising the crane and its drive system [8], [13], [14], and to examine selected types of control units and their settings. Fig. 5 shows the waveforms of selected co-ordinates of the model, obtained by numerical simulation of one of the considered control systems. These results inspired the author to verify experimentally the strategy of control of crane body slewing motion. For this purpose, one assumed the structure of the system consisting of two parts: the one generating the input signal $\varphi_{1\ zad}(t)$ based on the ULW structure (Fig 3, $R_2=0$) and the second one, the final control element, which has the structure of URP (Fig. 3, $R_1=0$). Block diagram of this system is shown in Fig. 6. One should consider the fact that hydraulic drive units in the system have aststic properties. On the other hand, the applied control units R_1 and R_2 are of PID type. One can notice then that the obtained waveform of $v_{rz}(t)$ will be similar to the input signal $v_{zad}(t)$ provided that mathematical model of the crane is equivalent to its physical model.

Consequently, the author constructed physical model of the crane equipped with a control unit for controlling angular position of the drive shaft. The model consists of the following parts

- jib, at the end of which the load is suspended along with a device used for measuring components of load swing,

- platform that simulates crane chassis together with a drive system allowing the part representing actual crane body to perform slewing motion,

- hydro-electric control system applied for controlling angle of rotation of the drive shaft [9], [12].

The jib is made of three segments with box-section of constant wall thickness, connected with telescopic lap joints facilitating the change of jib length. The angle of inclination can be adjusted by means of a screw simulating the hydraulic cylinder that controls the crane radius. Clearances in the joints of jib segments have been eliminated by application of teflon slippers. The jib is attached to the rotating plate by articulated joint.
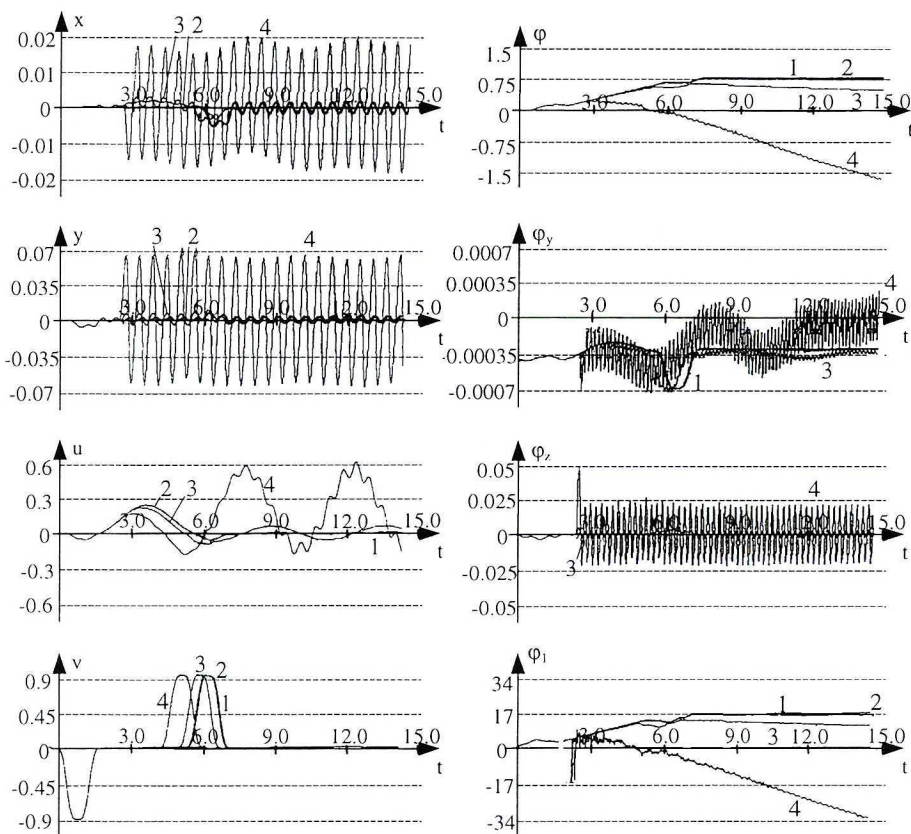
Fig. 5   Waveforms of selected state variables in the model of system of suppression of tangential component of load swing (pulse excitation, $F_n = F_{v0}[\mathbf{1}(t\text{-}\tau)\text{-}\mathbf{1}(t\text{-}\tau\text{-}\Delta t)]$, having the form of a horizontal force acting on the load, whose line of action passes through load centre of gravity and direction is consistent with that of the swing component v):

graphs 1: the case of operation without disturbances,

graphs 2: excitation parameters $F_{v0} = 1\text{kN}, \tau = 2.5\text{s}, \Delta t = 0.2\text{s}$,

graphs 3: excitation parameters $F_{v0} = 5\text{kN}, \tau = 2.5\text{s}, \Delta t = 0.2\text{s}$,

graphs 4: excitation parameters $F_{v0} = 50\text{kN}, \tau = 2.5\text{s}, \Delta t = 0.2\text{s}$.

The platform is a rectangular plate fixed to the substrate at its corners by means of vertical springs that simulate actual support system of the crane. The bearing of vertical drive shaft of the rotating plate is attached to the platform. A hydraulic engine drives the shaft by means of a closed transmission gear. Pulse gauge (encoder) placed on the shaft is used to measure shaft angle of rotation. The signal from encoder is applied as the feedback signal in the control system URP.
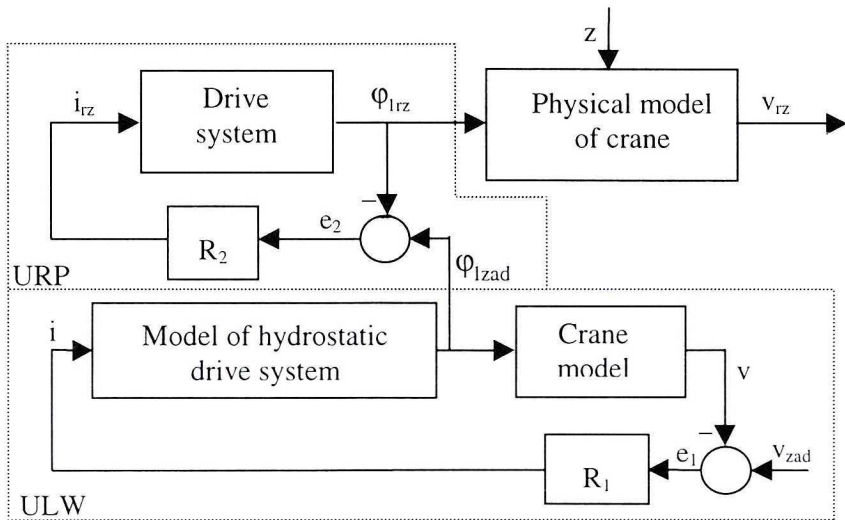
Fig. 6 Block diagram of control system used in experimental tests

The drive system comprises a gear pump of constant delivery, a hydraulic engine of constant capacity, and a proportional valve co-operating with a differential one; the proportional valve maintains constant pressure drop on the latter. Valve setting is done by means of electromagnetic motors controlled by the PCL controller through a digital-to-analog converter and current amplifier. The PLC controller plays the role of control unit in which the signal $\varphi_{1\,zad}$, generated numerically by simulation software, is compared with the signal measured by the encoder. Consequently, a control signal is produced due to the assumed PID-type function of the unit.

A special measuring device is placed in the upper part of the jib last segment. Its aim is to measure deflection of the hoisting rope in two perpendicular horizontal directions: in the vertical plane in which there lies undeformed axis of the jib (measurement of radial component of rope swing during slewing motion of the model), and in the plane perpendicular to the first one (measurement of tangential component of rope swing). The knowledge of these deflections makes it possible, after applying appropriate calibration procedure, to record waveforms of load swing components u and v, respectively.

The input signal $\varphi_{1\,zad}$ is the command signal in the system that controls angular position of engine drive shaft, URP (Fig. 6). The signal is generated by numerical simulation for the ULW system of suppression of component v of load swing. In creating the signal, one takes into account kinematic-geometric properties of the physical model. Fig. 7 shows waveforms of selected co-ordinates of the model obtained by numerical simulation, and the waveforms of corresponding quantities in the physical model, obtained experimentally [9].
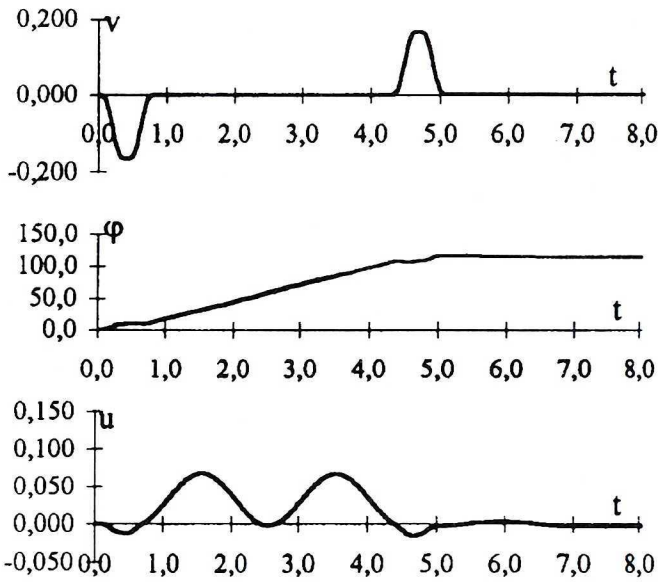
Fig. 7a Waveforms of selected co-ordinates of control system of crane slewing motion obtained by numerical simulation
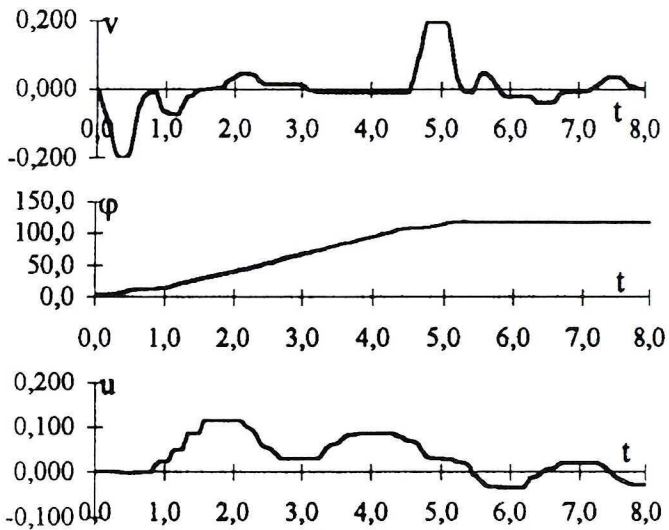
Fig.7b Waveforms of the same selected co-ordinates of control system of slewing motion of crane physical model, obtained experimentally

Despite nonlinearity existing in the physical model, and despite the assumed simplifications in the model of drive system, the result of experimental verification of the applied control strategy can be assessed positively.

4. Concluding remarks

The numerical and experimental investigations on the system of control of crane body movement, reported in this paper, indicate that a similar procedure could be applied to controlling the crane radius [11]. It can also be used in a system of combined control of both slewing motion of crane body and jib radius. That would make it possible to transport the load to a specified point while suppressing its oscillations. The problem of load positioning can also be extended to the case when working motion starts with a non-zero swing of the load [4].

The proposed method allows for controlling the movement of load suspension point in such a way that the load is carried to the selected point within the crane working area, and at the same time load swing is suppressed at the end of motion. Additionally, at certain moments, the speed of movement can reach maximum permissible values.

5. Acknowledgements

* * *

APPENDIX

Matrix M_1 has the following form:

$$\mathbf{M}_1 = \left\{ m_{i,j} \right\} \qquad i, j = 1, \ldots, 8,$$

where:

$$m_{1,1} = m_{2,2} = m_1 + m_2 + m_3 ,$$
$$m_{1,8} = m_{8,1} = -m_{ws} R_c \sin \varphi + m_3 d_4 ,$$

$$m_{1,3} = m_{3,1} = m_3 d_{11} ,$$
$$m_{2,3} = m_{3,2} = m_3 d_{13} ,$$

$$m_{1,4} = m_{4,1} = m_3 d_{12} ,$$
$$m_{2,4} = m_{4,2} = m_3 d_{14} ,$$

$$m_{1,5} = m_{5,1} = m_{ws} d_{19} + m_3 d_6 ,$$
$$m_{2,5} = m_{5,2} = m_{ws} d_{18} + m_3 d_7 ,$$

$$m_{1,7} = m_{7,1} = m_{nw} h_1 + m_{ws} d_{17} + m_3 d_1 ,$$
$$m_{2,6} = m_{6,2} = -m_{1,7} ,$$

$$m_{2,8} = m_{8,2} = m_{ws} R_c \cos \varphi + m_3 d_5 ,$$
$$m_{3,3} = m_3 \left(d_{11}^{\,2} + d_{13}^{\,2} + d_{15}^{\,2} \right) ,$$

$$m_{3,4} = m_{4,3} = m_3 \left(d_{11}d_{12} + d_{13}d_{14} + d_{15}d_{16} \right), \quad m_{3,6} = m_{6,3} = -m_3 \left(d_1 d_{13} + d_4 d_{15} \right),$$

$$m_{3,5} = m_{5,3} = m_3 \left(d_6 d_{11} + d_7 d_{13} + d_{15}d_{10} \right), \quad m_{3,7} = m_{7,3} = m_3 \left(d_1 d_{11} - d_5 d_{15} \right),$$

$$m_{3,8} = m_{8,3} = m_3 \left(d_4 d_{11} + d_5 d_{13} \right), \qquad m_{4,6} = m_{6,4} = -m_3 \left(d_1 d_{14} + d_4 d_{16} \right),$$

$$m_{4,4} = m_3 \left(d_{12}{}^2 + d_{14}{}^2 + d_{16}{}^2 \right), \qquad m_{4,7} = m_{7,4} = m_3 \left(d_1 d_{12} - d_5 d_{16} \right),$$

$$m_{4,5} = m_{5,4} = m_3 \left(d_6 d_{12} + d_7 d_{14} + d_{16}d_{10} \right), \quad m_{4,8} = m_{8,4} = m_3 \left(d_4 d_{12} + d_5 d_{14} \right),$$

$$m_{5,5} = J_{nwz} + J_{wsz} + m_{ws} \left(d_{18}{}^2 + d_{19}{}^2 + d_{20}{}^2 \right) + m_3 \left(d_6{}^2 + d_7{}^2 + d_{10}{}^2 \right),$$

$$m_{5,6} = m_{6,5} = m_{ws} \left(d_{20} R_c \sin \varphi - d_{17}d_{18} \right) - m_3 \left(d_1 d_7 + d_4 d_{10} \right),$$

$$m_{5,7} = m_{7,5} = m_{ws} \left(d_{17}d_{19} - d_{20} R_c \cos \varphi \right) + m_3 \left(d_1 d_6 - d_5 d_{10} \right),$$

$$m_{5,8} = m_{8,5} = J_{nwz} + J_{wsz} + m_{ws} \left(-d_{19} R_c \sin \varphi + d_{18} R_c \cos \varphi \right) +$$
$$+ m_3 \left(d_4 d_6 + d_5 d_7 \right),$$

$$m_{6,6} = J_x + J_{nwx} + J_{wsx} + m_{nw} h_1{}^2 + m_{ws} \left(d_{17}{}^2 + R_c{}^2 \sin^2 \varphi \right) + m_3 \left(d_1{}^2 + d_4{}^2 \right),$$

$$m_{6,7} = m_{7,6} = -m_{ws} R_c{}^2 \sin \varphi \cos \varphi + m_3 d_4 d_5 ,$$

$$m_{6,8} = m_{8,6} = -m_{ws} d_{17} R_c \cos \varphi + m_3 d_1 d_5 ,$$

$$m_{7,7} = J_y + J_{nwy} + J_{wsy} + m_{nw} h_1{}^2 + m_{ws} \left(d_{17}{}^2 + R_c{}^2 \cos^2 \varphi \right) + m_3 \left(d_1{}^2 + d_5{}^2 \right),$$

$$m_{7,8} = m_{8,7} = -m_{ws} d_{17} R_c \sin \varphi + m_3 d_1 d_4 ,$$

$$m_{8,8} = J_z + J_{nwz} + J_{wsz} + m_{ws} R_c{}^2 + m_3 \left(d_4{}^2 + d_5{}^2 \right);$$

The remaining elements of matrix M_1 are equal to 0;

$$d_1 = h + l_w \sin \kappa - \sqrt{l^2 - u^2 - v^2} \qquad\qquad R_c = l_c \cos \kappa - b_n$$

$$d_2 = \cos \varphi - \varphi_z \sin \varphi , \qquad\qquad d_5 = -v \sin \varphi + (R + u) \cos \varphi ,$$

$$d_3 = -\varphi_z \cos \varphi - \sin \varphi , \qquad\qquad d_6 = -v d_2 + (R + u) d_3 ,$$

$$d_4 = -v \cos \varphi - (R + u) \sin \varphi , \qquad\qquad d_7 = v d_3 + (R + u) d_2 ,$$

$$d_8 = \varphi_x \sin \varphi - \varphi_y \cos \varphi , \qquad\qquad d_9 = \varphi_x \cos \varphi + \varphi_y \sin \varphi ,$$

$$d_{10} = (R + u) d_9 - v d_8 , \qquad\qquad R = l_w \cos \kappa - b_n$$

$$d_{11} = d_2 + \frac{u \varphi_y}{\sqrt{l^2 - u^2 - v^2}} , \qquad\qquad d_{14} = d_2 - \frac{v \varphi_x}{\sqrt{l^2 - u^2 - v^2}} ,$$

$$d_{12} = d_3 + \frac{v \varphi_y}{\sqrt{l^2 - u^2 - v^2}} , \qquad\qquad d_{15} = d_8 + \frac{u}{\sqrt{l^2 - u^2 - v^2}} ,$$

$$d_{13} = -d_3 - \frac{u \varphi_x}{\sqrt{l^2 - u^2 - v^2}} , \qquad\qquad d_{16} = d_9 + \frac{v}{\sqrt{l^2 - u^2 - v^2}} ,$$

$$d_{17} = h + l_c \sin \kappa \, , \qquad\qquad d_{19} = -R_c \sin \varphi - \varphi_z R_c \cos \varphi \, ,$$

$$d_{18} = R_c \cos \varphi - \varphi_z R_c \sin \varphi \, , \qquad d_{20} = R_c \varphi_x \cos \varphi + R_c \varphi_y \sin \varphi \, .$$

Matrix $\mathbf{C}_{p1}$ and vector $\mathbf{c}_{r1}$ have the following forms:

$$\mathbf{C}_{p1} = \left\{ c_{pi.j} \right\} \qquad i, j = 1, 2, ..., 8;$$

$$\mathbf{c}_{r1} = \left\{ c_{r1i} \right\} \qquad i = 1, 2, ..., 8;$$

where:

$$c_{p1.1} = 4k_x \, , \qquad\qquad\qquad c_{p5.5} = -c_{p5.8} = -c_{p8.5} = k_{sp} \, ,$$

$$c_{p2.2} = 4k_y \, , \qquad\qquad\qquad c_{p6.6} = 4k_z a^2 \, ,$$

$$c_{p2.8} = c_{p8.2} = 2k_y \left(b - c \right) , \qquad\qquad c_{p7.7} = 2k_z \left(b^2 + c^2 \right) ,$$

$$c_{p3.6} = c_{p6.3} = c_{p4.7} = c_{p7.4} = m_3 g \sin \varphi \, , \qquad c_{p8.8} = 4k_x a^2 + 2k_y \left(b^2 + c^2 \right) + k_{sp} \, ,$$

$$c_{p3.7} = c_{p7.3} = -c_{p4.6} = -c_{p6.4} = -m_3 g \cos \varphi \, ;$$

$$c_{r15} = -c_{r18} = -i_p \varphi_1 k_{sp} \, ,$$

$$c_{r16} = ak_z \left(z_{1st} - z_{2st} + z_{3st} - z_{4st} \right) + \left(m_3 gR + m_{ws} gR_c \right) \sin \varphi \, ,$$

$$c_{r17} = bk_z \left(z_{1st} + z_{2st} \right) - ck_z \left(z_{3st} + z_{4st} \right) - \left(m_3 gR + m_{ws} gR_c \right) \cos \varphi \, ;$$

The remaining elements of matrix $\mathbf{C}_{p1}$ and vector $\mathbf{c}_{r1}$ are equal to 0;
The quantity c_{s1} has the following form:

$$c_{s1} = \frac{1}{2} k_z \left(z_{1st}^2 + z_{2st}^2 + z_{3st}^2 + z_{4st}^2 \right) + \frac{1}{2} k_{sp} i_p^2 \varphi_1^2 + m_{nw} gh_1 +$$

$$+ m_{ws} g \left(h + l_c \sin \kappa \right) + m_3 g d_1 \, .$$

The following symbols are used in the formulas:

m_1, m_2, m_3, m_{nw}, m_{ws} – mass of chassis, mass of body with jib, mass of load, mass of crane body and mass of jib, respectively,

J_x, J_y, J_z, J_{nwx}, J_{nwy}, J_{nwz}, J_{wsx}, J_{wsy}, J_{wsz} - moments of inertia of chassis, of crane body and of jib with reference to x, y and z axes,

a, b, c, b_n, l_w, l_c, h, h_1 – dimensions of crane model according to Fig.1,

z_{1st}, z_{2st}, z_{3st}, z_{4st} – vertical displacements of springs modelling the bearing system,

l – length of hoisting rope,

g – acceleration of gravity;

The remaining symbols are described in the main body of the text.

REFERENCES

[1]   Auernig J.W.: Einfache Steuerstrategien für Laufkatzkrane zur Vermeidung des Lastpendelns im Zielpunkt. Fordern und Heben, 1986, No 6, p. 413÷420.

[2]   Jedliński W.: The problem of creating the discrete dynamic model of tower crane (in Polish). The Archive of Mechanical Engineering (ABM), 1970, Vol. XVII, z. 4.

[3]   Kłosiński J.: Simulative investigations on mobile crane jib taking into account suppression of load oscillations at the end point (in Polish). Proceedings of the PIMB, International Scientific Conference: "Development of Design and Test of Mobile, Hydraulic Cranes", Warszawa–Zaborów 1992, v. 2-5, pp. 143÷150.

[4]   Kłosiński J.: An analysis of possibilities of controlling working motion of a crane truck (in Polish). Zeszyty Naukowe PŁ Filii w Bielsku-Białej. Budowa i Eksploatacja Maszyn, 1993, z. 13, No 14.

[5]   Kłosiński J.: Displacements of crane chassis as a disturbance in work of the system controlling working motion of crane truck (in Polish). Dozór Techniczny 1994, No 5.

[6]   Kłosiński J.: A method for determining the controlling strategy of crane truck slewing motion (in Polish). Proceedings of the XIV National Conference on Theory of Machines and Mechanisms. Gdańsk 1994, p. 167÷172.

[7]   Kłosiński J.: Selection of input signal used to control slewing motion of a truck crane (in Polish). Proc. of the XI Conference "Problems of Development of Heavy Machinery" Warszawa-Zakopane 1998, p. 197÷204.

[8]   Kłosiński J.: The influence of disturbance signals on the systems controlling the working motions of a crane truck model (in Polish). Proceedings of the XVI National Conference on Theory of Machines and Mechanisms. Rzeszów-Solina 1998.

[9]   Kłosiński J., Janusz J.: Experimental verification of the algorithm of slewing motion control in mobile crane physical model (in Polish). Proceedings of the IV Conference on Experimental Methods in Development and Exploitation of Machinery. Wrocław-Szklarska Poręba 1999.

[10]   Pizoń A.: Elektrohydrauliczne analogowe i cyfrowe układy automatyki. WNT, Warszawa 1995 (in Polish)

[11]   Trombski M., Kłosiński J., Majewski L., Suwaj S.: Automation of working motion control in mobile working machines (in Polish). The presentation of research projects on robotics and machine and mechanism theory, sponsored by the KBN. Gdańsk 1994, p. 69÷77.

[12]   Trombski M., Kłosiński J., Majewski L., Suwaj S.: A physical model of crane truck applied to simulation of controlling the slewing motion (in Polish). Proceedings of the II Conference on Experimental Methods in Development and Exploitation of Machinery. Wrocław-Szklarska Poręba 1995, p. 341÷346.

[13]   Trombski M., Kłosiński J., Majewski L., Suwaj S.: Some Problems of Controlling Crane Truck Working Movements. Proceedings of the IXth World Congress on the Theory of Machines and Mechanisms. Milan 1995. v.2, p. 1411÷1415.

[14]   Trombski M., Kłosiński J., Majewski L., Suwaj S.: Sensitivity of the Systems Controlling the Working Motions of a Mobile Crane to the Disturbance Signals, Proceedings of the Xth World Congress on the Theory of Machines and Mechanism, v. 4, pp. 1578÷1583, Oulu 1999.

[15]   Valasek M.: Programove rizeni jerabu v realnem case (in Czech). Automatizace 29 (1986) pt. 8-9, p. 211÷215.

[16]   Zrnic D., Bugaric U., Vukovic J.: The Optimization of Moving Cycle of Grab by Unloading Bridges. Proceedings of the IXth World Congress on the Theory of Machines and Mechanisms. Milan 1995, p. 1001÷1005.

Sterowanie ruchem obrotowym żurawia teleskopowego zapewniające pozycjonowanie przenoszonego ładunku

Streszczenie

W pracy przedstawiono algorytm sterowania ruchem obrotowym żurawia teleskopowego na podwoziu samochodowym zapewniającego przeniesienie ładunku do określonego punktu łącznie z likwidacją jego wahań po zakończeniu ruchu roboczego. Na sterowaniu ruchem obrotowym nadwozia żurawia skupiono szczególną uwagę, głównie ze względu na niepłaski rozkład sił obciążających ładunek w trakcie jego ruchu. W tym celu zbudowano uproszczone modele żurawia i jego hydraulicznego układu napędowego, następnie dokonano analitycznej identyfikacji obu modeli. Traktując oba modele jako obiekt regulacji zaproponowano strukturę układu regulacji tej składowej wahań ładunku, która leży na kierunku stycznym do toru wykreślanego przez punkt zawieszenia ładunku. Symulacje numeryczne modelu matematycznego układu regulacji uzupełniono eksperymentem na modelu fizycznym żurawia, celem eksperymentu była weryfikacja strategii sterującej w sensie jej przydatności w zastosowaniach technicznych.